

# Real-time resolving assembly graph by ONT long reads data

Son Hoang Nguyen<sup>1,\*</sup>, Minh Duc Cao<sup>2</sup>, and Lachlan Coin<sup>1,\*</sup>

<sup>1</sup>Institute for Molecular Bioscience, the University of Queensland, St Lucia, Brisbane, QLD 4072 Australia; <sup>2</sup>4catalyzer

\* To whom correspondence should be addressed. E-mails: l.coin@imb.uq.edu.au, s.hoangnguyen@imb.uq.edu.au

5

This manuscript was compiled on **November 15, 2019 16:54**

**Abstract:** A real-time assembly pipeline for Oxford Nanopore Technology (ONT) data is important for either saving sequencing resources or reducing turnaround time for data analyses. The previous approach from **npScarf** provided a greedy fast-response, auto-correct streaming algorithm for such task but was relatively prone to mis-assemblies compared to other graph-based methods. Here we present **npGraph**, a real-time hybrid assembly software using the assembly graph instead of the separated pre-assembly contigs. It is able to produce more complete genome assembly by resolving the path finding problem on the assembly graph using long reads as the traversing guide. The applications on synthetic and real data set of isolate genomes show improved accuracy while still maintain the required computational cost at very low level. In addition, the GUI feature can provide users a comprehensive look-and-feel of the whole assembly process. The tool and source code is available at <https://github.com/hsnguyen/assembly>.

**Keywords:** hybrid assembly, assembly graph, real-time analysis, nanopore sequencing

## Introduction

Streaming assembly methods have been proven to be useful in saving time and resources compared to the traditional batch algorithms with examples included *e.g.* **Faucet** [1] and **npScarf** [2]. The first method allows the assembly graph to be constructed incrementally as long as reads are retrieved and processed. This practice is helpful dealing with huge short-read data set because it can significantly reduce the local storage for the reads, as well as save time for a DBG construction while waiting for the data being retrieved.

10

**npScarf**, on the other hand, works on the available short-read assembly to scaffold the contigs using nanopore sequencing which is well-known by the real-time property. The completion of genome assembly along with the sequencing run provides explicit benefits in term of resource control and turn-around time for analysis [2]. However, due to the greedy approach of a streaming algorithm, as well as being an alignment-based-only scaffolding mechanism, running the tool with default settings suffers from mis-assemblies [3, 4]. In many case, the gap filling step has to rely on the low quality nanopore reads thus the accuracy of the final assembly is affected as well. To tackle the quality issue while maintaining its streaming execution, an assembly graph processing system is investigated as it would provide an additional high-quality source of linking information for the assembly operations.

15

20

After the construction of an assembly graph, the next step is to traverse the graph, resolve the repeats and identify the longest possible un-branched paths that would represents contigs for the final assembly. Hybrid assembler using nanopore data to resolve the graph has been implemented in **hybridSPAdes** [5] or **Unicycler** [3]. In general, the available tools employ batch-mode algorithms on the whole long-read data set to generate the final genome assembly. In which, the **SPAdes** hybrid assembly module, from its first step, exhaustively looks for the most likely paths (with minimum edit distance) on the graph for each of the long read given but only ones supported by at least two reads are attained. In the next step, these paths will be subjected to a decision-rule algorithm, namely **exSPAndeR** [6], for repeat resolution by step-by-step expansion, before output the final assembly. On the other hand, **Unicycler**'s hybrid assembler will initially generate a consensus long read for each of the bridge from the batch data. The higher quality consensus reads are used to align with the assembly graph to find the best paths bridging pairs of anchored contigs. While the later approach employs the completeness of the data set from the very beginning for a consensus step, the former only iterates over the batch of possible paths and relies on a scoring system for the final decision of graph traversal. For that reason, the first direction is more suitable for a real-time pipeline.

25

30

35

However, the challenges to adapt this approach into a real-time mechanism are obvious and mainly come from the heavy path-finding task and the complication of self-improvement step which is critical to a streaming algorithm. A modified DFS algorithm and a voting system with accumulating scores calculation has been implemented to overcome these issues. This results in **npGraph**, an user-friendly tool with GUI that can traverse the assembly graph and scaffold its components in real-time as long as the nanopore sequencing process is running and continuously generating long reads.

40

## Results

### npGraph – a tool to resolve assembly graph in real-time

npGraph's input consists of Illumina assembly graph resulted from running assembler, e.g. SPAdes [7], Velvet [8], AbySS [9] on Illumina short reads, together with long reads from third generation sequencing technology (Oxford Nanopore Technology, Pacbio). The long reads will be aligned with the contigs in the assembly graph to indicate longer paths that should be traversed. These local paths, given sufficient data, are expected to untangle the complicated graph and guide to the global Eulerian paths (or cycles if possible) that represent the entire genomic sequences. npGraph can be invoked and fully function from the command-line interface. In addition, in order to aid the visualization of the assembly process, a GUI has been developed as well.

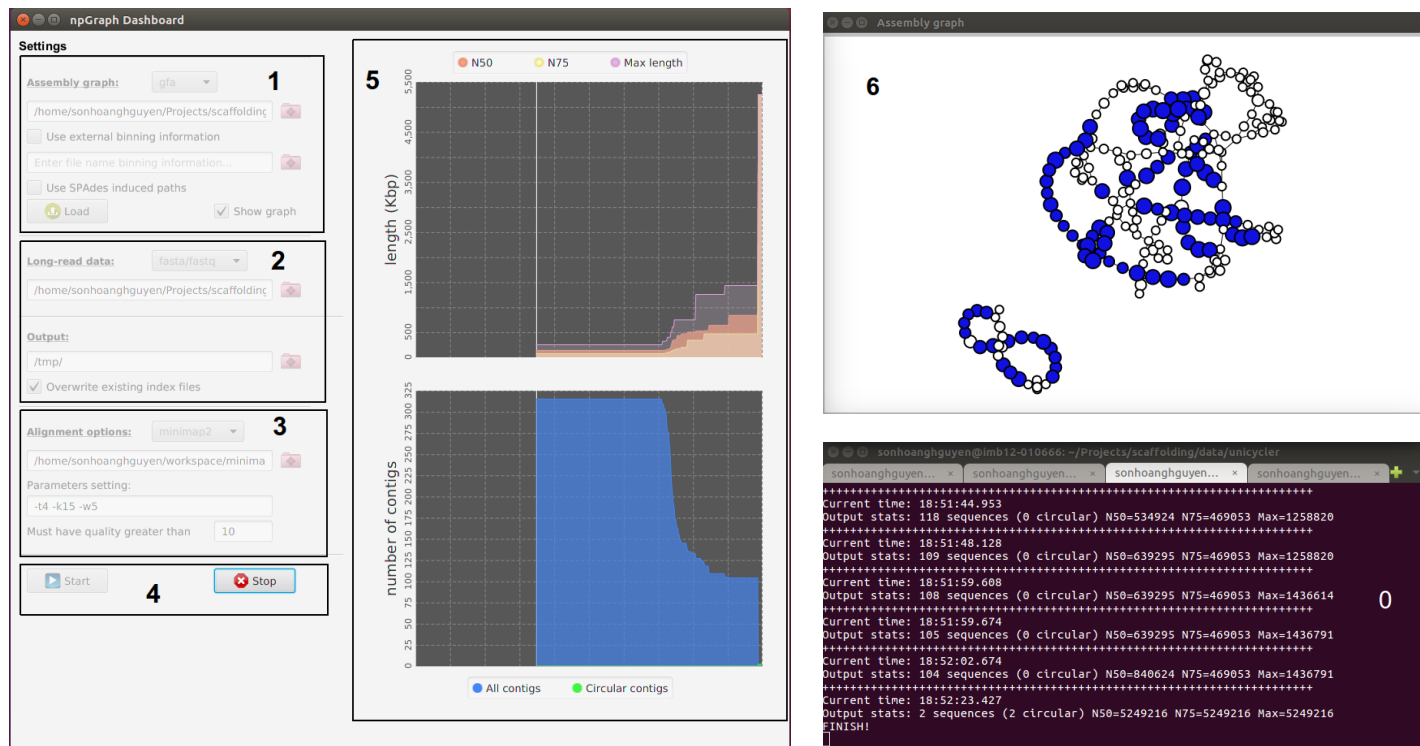


Figure 1: npGraph user interface including Console (0) and GUI components (1-6). The GUI consists of the Dashboard (1-5) and the Graph View (6). From the Dashboard there are 5 components as follow: 1 the assembly graph input field; 2 the long reads input field; 3 the aligner settings field; 4 control buttons (start/stop) to monitor the real-time scaffolding process; 5 the statistics plots for the assembly result.

The GUI includes the dashboard for control the settings of the program and another pop-up window for a simple visualization of the assembly graph in real-time (Figure 1). In this interface, the assembly graph loading stage is separated from the actual assembly process so that users can check for the graph quality first before carry out any further tasks. The box numbered 1 on Figure 1 is designed for this task. Only after an assembly graph is loaded successfully, users can move to box 2 to specify the nanopore input data. Settings for an aligner (BWA-MEM or minimap2) in box 3 is required if the input is the raw sequences in FASTA/FASTQ format. Another option is to run the alignment independently and provide SAM/BAM input for the next stage of bridging and assembly. This stage is controlled by buttons in box 4: the START button ignites the process while the STOP button can prematurely terminate it and output the assembly result till that moment. The plots from the right panel (5) depicts real-time statistics of the assembly contigs inferred from the graph. From the second window (6), the colored vertices imply unique contigs while the white ones involve either unspecified or repetitive elements. The number of different colors (other than white) indicates the amount of abundant groups being detected as population bins (e.g. chromosome versus different plasmids, or different bins in metagenomics).

A proper combination of command line and GUI can provide an useful streaming pipeline that copes well with MinION output data. The practice is similar to the previous developed pipelines [2, 10, 11] that allow the analysis to take place abreast to a nanopore sequencing run.

### Hybrid assembly for synthetic data sets

To evaluate the performance of the method, npGraph was benchmarked against SPAdes with its hybrid assembly module [5], npScarf with/without assembly graph integrated, and Unicycler version 0.4.6 on the latter's testing data [3]

. This data set were simulations of Illumina and MinION raw data, generated *in silico* based on random and available microbial references. Specifically, the synthetic Illumina data was generated by using a wrapper script of ART [12] that allows uniform coverage for circular genome sequencing with justifiable depths. PBSIM [13], on the other hand, was used to simulate the long reads.

There were three settings for each of the synthetic raw data (*good*, *medium*, *bad*) corresponding to the quality, yield and length of reads being generated. In the SGS simulation, the *bad* data consist of 100bp paired-end reads with low and uneven coverage (40X) leading to many dead ends in the assembly graph due to missing regions in the genome. The read length was 125bp in the *medium* setting with better depth distributions that could cover the genome better. Finally, the *good* option provided best data sets with 150bp of read length and 100X coverage. While the quality of SGS reads would determine the assembly graph nature, the nanopore data plays critical role in graph resolving. The three settings leveled up the depth (8X, 16X, 32X) and at the same time, average length (5Kbp, 10Kbp, 20Kbp) and maximum identities (90% ,95% ,98%) respectively. We only considered the *good* configurations of both platforms for the sequence data being tested. Also, since the other comparative tools do not support streaming assembly, there were only batch-mode runs being carried out and the reciprocal results were examined by QUAST 5.0.2 [14].

Table 1: Comparison of assemblies produced in batch-mode using npGraph and the comparative methods on 5 synthetic data sets taken from <https://cloudstor.aarnet.edu.au/plus/index.php/s/dzRCaxLjpGpfKYW>

Method	Assembly size (Mb)	#Contigs	N50 (Kp)	Mis-assemblies	Error (per 100 Kb)	Run times (CPU hrs)
random sequence with repeats						
SPAdes	3.928	226	40.5	0	0.00	0.95
SPAdes-Hybrid	4.109	3	4,000.0	0	0.85	1.196
Unicycler	4.110	3	4,000.0	0	0.47	6.783
npScarf	4.251	9	3,952.2	27	8.74	0.95 + 0.39
npScarf_wag	4.554	9	3,999.6	37	6.16	0.95 + 0.45
npGraph (bwa)	4.110	3	4,000.0	0	0.47	0.95 + 0.33
ngGraph (minimap2)	4.110	3	4,000.0	0	0.47	0.95 + 0.02
<i>Mycobacterium tuberculosis</i> H37Rv						
SPAdes	4.371	114	125.5	1	1.51	1.55
SPAdes-Hybrid	4.411	1	4,411.2	0	1.73	1.68
Unicycler	4.412	1	4,411.5	0	2.56	6.36
npScarf	4.446	4	4,389.9	12	11.41	1.55 + 0.78
npScarf_wag	4.408	1	4,407.6	2	7.01	1.55 + 0.79
npGraph (bwa)	4.411	1	4,411.6	0	7.28	1.55 + 0.63
ngGraph (minimap2)	4.411	1	4,411.4	0	7.01	1.55 + 0.02
<i>E. coli</i> O25b H4-ST131						
SPAdes	5.173	159	191.0	1	1.69	1.26
SPAdes-Hybrid	5.249	7	5,109.6	0	2.65	1.40
Unicycler	5.249	3	5,109.8	0	4.29	4.70
npScarf	5.354	7	5,087.5	14	29.12	1.26 + 0.78
npScarf_wag	5.413	7	5,108.1	6	30.29	1.26 + 0.78
npGraph (bwa)	5.252	3	5,112.3	0	16.37	1.26 + 0.66
ngGraph (minimap2)	5.250	3	5,111.1	0	14.61	1.26 + 0.03
<i>Streptococcus suis</i> BM407						
SPAdes	2.119	81	131.0	0	3.84	0.59
SPAdes-Hybrid	2.147	48	1,438.0	0	0.98	0.65
Unicycler	2.171	2	2,146.2	0	2.99	2.58
npScarf	2.220	4	2,120.0	9	97.20	0.59 + 0.31
npScarf_wag	2.245	4	2,128.3	3	89.64	0.59 + 0.31
npGraph (bwa)	2.167	6	2,146.7	0	26.77	0.59 + 0.21
ngGraph (minimap2)	2.167	6	2,146.2	0	22.53	0.59 + 0.01
<i>Acinetobacter</i> AB30						
SPAdes	4.134	265	42.5	0	3.23	0.95
SPAdes-Hybrid	4.287	49	3,308.0	0	5.04	1.84
Unicycler	4.333	1	4,333.0	1	6.95	5.27
npScarf	4.595	11	4,299.7	1	120.99	0.95 + 0.45
npScarf_wag	-	-	-	-	-	-
npGraph (bwa)	4.317	6	2,766.9	1	39.82	0.95 + 0.41
ngGraph (minimap2)	4.337	1	4,336.8	0	24.71	0.95 + 0.03

Table 1 shows evaluation results for 5 synthetic data sets, the output of the full run can be found in Supplementary Table 1. In the first column of applied methods, beside **Unicycler** and **hybridSPAdes**, the original scaffolder **npScarf** was included as well as **npScarf\_wag** – its modified version with assembly graph integrated. On the other hand, **npGraph** can use 2 different aligners, **BWA-MEM** and **minimap2**, for its bridging phase thus both practices were included in this comparison.

In general, the graph integrated version of **npScarf** improved the assembly results in terms of mis-assemblies and error reduction while virtually consuming similar resources compared to the original version. The only exception where the number of mis-assemblies being increased was the simulation of a random sequence with many repeats. There were 10 more mistakes detected using the later version **npScarf\_wag**. However, with additional investigations, we found that the number of mis-assemblies on the true positive circular sequences (3 from the reference) has been significant reduced by applying assembly graph for **npScarf**. The errors mostly came from redundant sequences output from the software due to the failure in estimation of contig multiplicity. Even though using assembly graph for gap fillings, there were no changes in the way to determine if a contig is unique or not from **npScarf\_wag**. It still relied on the length and coverage statistics, *i.e.* **Astats** [15] to find anchors that were critical for the backbone construction of the assembly. Redundant path findings for false positive replicons consequently returned additional wrong translocations in the final contigs which were reported by **QUAST**. Other than that, the method had successfully produced better assemblies than the original. Regarding *Mycobacterium tuberculosis* H37Rv, the number of mis-assembled breakpoints had been trimmed down from 12 to 2, while the number of final contigs had reduced from 4 to only one as in the reference. Results in cases of *E. coli* O25b H4ST131 and *Streptococcus suis* BM407 also showed enhancements in terms of those categories as well as N50 statistics. There was improvements considering the nucleotide errors (mismatches and indels) as well from aforementioned data sets, except for the *E. coli* when slightly more mismatches had been detected. However, these errors can be corrected by running polishing tools with the raw Illumina data afterward.

For *Acinetobacter* AB30 synthetic data, it was an deficiency for **npScarf\_wag** in traversing the graph to find candidate paths for a bridge of long distance due to particular large search space. The exhaustive, naive DFS implementation for this version of **npScarf** required a lot of memory to traverse a complex assembly graph that usually exceed a normal desktop's capacity. This issue has been fixed in **npGraph** when Algorithm 1 was used on the definitive graph. This resulted in completed runs of the assembly process for all data sets with the similar number of mis-assemblies compared to the best figures in this category. As shown in Table 1 and 1, the assembly graph based methods offered significant improvements when compared to **npScarf**. Not only because of the clear drops with respect to mis-assemblies and errors, but it was also reflected by the number of final contigs and their N50 as well.

To align the long reads to the assembly graph components, either **BWA-MEM** [16] or **minimap2** [17] was invoked in **npGraph**. The former option was inherited from **npScarf** pipeline with the intact parameters while the latter was used with the recommended settings (-k15 -w5) for the best sensitivity working on MinION data. Even though, **BWA-MEM** normally reported more hits than **minimap2** but at the same time, was responsible for more false positive alignments. For instance, regarding the last data set from Table 1, the assembly of **npGraph** using **BWA-MEM** was suffered from the ambiguous alignments thus more fragmented than the other counterparts. On the other hand, referring to more complicated graphs from *Acinetobacter* A1 and the yeast *Saccharomyces cerevisiae* S288c from Table 1, the number of mis-assemblies from using **minimap2** were increased due to the lacks of appropriate alignments to support accurate bridging process. However, under almost circumstances, using either aligners would result in final assemblies with similar qualities. Furthermore, in terms of running time and resources required, **minimap2** proved to be the best option. The total CPU hours had been trimmed down drastically with the new aligner, making **npGraph** the fastest hybrid assembler available. This feature is certainly more favoured to a real-time assembly as well. As the consequence, as long as **minimap2** is expected to replace **BWA-MEM** for long-read sequencing data alignment, it would likewise become the main aligner for **npGraph** pipeline in the future.

It is noteworthy to discuss in more details the errors addressed in the above assembly methods. This figure measured the total mismatches and indels per 100kbp from the assembly sequences when mapping to the reference. As expected from hybrid assemblies where Illumina sequencing data were used as the main building blocks, the figures were hardly bigger than 100 (equivalent to 0.1% error rate) for almost every case. In addition, the indels errors, which mainly caused by TGS data, were found relatively low in the final contigs (Table 1). The majority of the differences accounted for the mismatched nucleotides caused by the alternative paths connecting the unique anchors from the backbone of the assembly. This phenomenon may root from homologous repeats or sequencing errors of the genome. From all the hybrid assemblers, **hybridSPAdes** reported results with highest fidelity. This meant that the performance its decision-rule algorithm **exSPAnDer** [6] was the most accurate amongst all path finding methods. As the trade-off, there were fewer connections satisfying its quality threshold, resulting in the fragmented assemblies in cases of *Streptococcus suis* or *Acinetobacter* samples (Table 1 and 1). **Unicycler**, which employs an algorithm based on semi-global (or glocal) alignments [18] with the consensus long reads, returned the second best reliable and at the same time, closest-to-complete results overall. **npScarf**, on the other hand, exploited the long reads for the gap filling thus inherited the high error rates from them. By integrating the assembly graph for the task, the errors were reduced in general (random sequences, *M. tuberculosis*, *S. suis* from Table 1) but not completely since the mis-placed contigs were still not resolved in other circumstances. **npGraph** significantly reduced the errors compared to **npScarf**, however the figures were still higher than the those of the best counterparts. This implied a more robust decision making system is needed in **npGraph**'s



real-time path finding module for even better output's accuracy.

### Hybrid assembly for real data sets

Several sequencing data sets of actual bacterial samples [19] were used in this scenario. The data included both Illumina paired-end and MinION sequencing based-call data for each sample. Unlike previous settings, rather than the default output, the optimal SPAdes assembly graph detected by Unicycler were used for npGraph algorithm as well. This step had been proved to be useful in selecting the best graph available, amongst SPAdes runs with ranging  $k$ -mer values, that have dead-ends and number of contigs minimized [3]. Likewise, as mentioned before, the quality of the initial assembly graph would considerably influence the final results of npGraph.

Due to the lack of available reference genomes, fewer statistics were reported by QUAST for the comparison of the results. Instead, we investigated the number of circular sequences and PlasmidFinder 1.3 [20] mappings to obtain an evaluation on the accuracy and completeness of the assemblies. Table 2 shows the benchmark results of npGraph (using minimap2) against Unicycler on three data sets of bacterial species *Citrobacter freundii*, *Enterobacter cloacae* and *Klebsiella oxytoca*.

Table 2: Assembly of real data sets using Unicycler and npGraph with the optimized SPAdes output. Circular contigs are highlighted in **bold**, fragmented assemblies are presented as X|Y where X is the total length and Y is the number of supposed contigs making up X.

	Unicycler	npGraph	Replicons (based on PlasmidFinder 1.3)
<i>Citrobacter freundii</i> CAV1374	<b>5,029,534</b>	<b>5,029,486</b>	Chromosome
	<b>109688</b>	<b>109688</b>	IncFIB(pHCM2)_1_pHCM2_AL513384
	<b>100,873</b>	<b>100,873</b>	IncFIB(pB171)_1_pB171_AB024946
	<b>85,575</b>	<b>85,575</b>	IncL/M(pMU407)_1_pMU407_U27345
	<b>43,621</b>	<b>43,621</b>	repA_1_pKPC-2_CP013325
	<b>3,223</b>	<b>3,223</b>	-
	<b>1,916</b>	<b>1,916</b>	ColRNAI_1_DQ298019
	14,464 3	14,456 2	-
<i>Enterobacter cloacae</i> CAV1411	4,806,666 2	4,858,438 2	Chromosome
	<b>90,451</b>	90,693 2	IncR_1_DQ449578
	<b>33,610</b>	<b>33,610</b>	repA_1_pKPC-2_CP013325
	13,129 2	14,542 4	-
<i>Klebsiella oxytoca</i> CAV1015	6,153,947 5	<b>6,155,762</b>	Chromosome
	<b>113,105</b>	<b>113,105</b>	IncFII(SARC14)_1_SARC14_JQ418540;
			IncFII(S)_1_CP000858
	<b>111,395</b>	<b>111,395</b>	-
	<b>108,418</b>	109,209 13	IncFIB(K)_1_Kpn3_JN233704
	<b>76,183</b>	<b>76,186</b>	IncL/M(pMU407)_1_pMU407_U27345
	<b>11,638</b>	11,892 2	-

From the first data set, there was high similarity between final contigs generated by two assemblers. They shared the same number of circular ultimate sequences, including the chromosomal and other six replicons contigs. The only divergence lied on the biggest sequence ( $\simeq 5.029$ Mbp) when the Unicycler's chromosome was 48 nucleotides longer than that of npGraph. Five out of six identical replicons were confirmed as plasmids based on the occurrences of appropriate Origin of replication sequences (PlasmidFinder database). In detail, two megaplasmids (longer than 100Kbp) were classified as IncFIB while the other two mid-size replicons, 85.6Kbp and 43.6Kbp, were incL and repA respectively, leaving the shortest one with 2Kbp of length as ColRNAI plasmid. The remaining circular sequence without any hits to the database was 3.2Kbp long suggesting that it could be phage or newly replicon's DNA. Lastly, there were still 14.5Kbp unfinished sequences resulted in 3 linear contigs from Unicycler and 2 for npGraph respectively.

The assembly task for *Enterobacter cloacae* was more challenging as the chromosomal DNA sequence was not been fully resolved using either method. The chromosome size was estimated to be approximately 4.8Mbp but had been broken into two smaller pieces. npGraph returned longer stretches of length 3.324Mbp and 1.534Mbp while the figures were 2.829Mbp and 1.978Mbp from Unicycler's output. However, the number of circular sequences detected by Unicycler was one more than the other (2 versus 1). They were corresponding to 2 plasmids, namely IncR and repA. While the latter were recognized by both methods, the longer plasmid sequence was fragmented running npGraph. Similar to the previous data set, there were around 14Kbp of data were unable to be finished by the assemblers.

Finally, assembly for *Klebsiella oxytoca* saw fragmented chromosome using Unicycler but it was a fully complete contig for npGraph with 6.156Mbp of size. The two assemblers shared 3 common circular sequences where two of them were confirmed plasmids. The first identical sequences represented a megaplasmid ( $\simeq 113$ Kbp) with two variations of IncFII's origin of replication DNA being identified. The other agreed plasmid were IncL/M with 76Kbp of length. Particularly, there was one circular contig with length greater than 100Kbp but returned no hits to the plasmid database,

suggesting the importance of *de novo* replicon assembly in combination with further interrogations. **Unicycler** detected another megaplasmid of size 108.4Kbp which was fractured by **npGraph**. The dissolution was also observed in **npGraph** for the final contig of length 11.6Kbp where it failed to combine two smaller sequences into one.

In addition to what presented in Table 2, dot plots for the pair-wise alignments between the assembly contigs were generated and can be found in Appendix Figure 1. Interestingly, beside all other agreements, there was a structural difference using two methods for *E. cloacae* CAV1411 genome assembly. This was caused by the inconsistency of a fragment's direction on the final output contigs. However, when compare to a reference genome of the same bacteria strain (GenBank ID: CP011581.1 [21]), contigs generated by **npGraph** demonstrated a consistent alignment which was not the case for **Unicycler** results (Appendix Figure 2). Even though this might reflect a novel variation between bacterial samples of the same strain, it was more likely a mis-assembly by using **Unicycler**.

Overall, by testing with synthetic and real data, **npGraph** proved to be able to generate assemblies of comparative quality compared to other powerful batch-mode hybrid assemblers, such as **hybridSPAdes** or **Unicycler**. Furthermore, similar to **npScarf**, it has the advantage in term of supporting real-time assembly. The next section will address this utility and the interactive GUI bundled in **npGraph**.

## Real-time mode hybrid assembly

Figure 2 demonstrates the real-time mode performance of **npScarf** and **npGraph** via N50 statistics during the assembly of 4 example data sets. This experiment would discover the rate of completing genome assemblies of the new method, set aside the accuracy aspect which had already been discussed previously. **npScarf\_wag** basically scaffolds the pre-assembly contigs in the same manner with the original version thus was not discussed here.

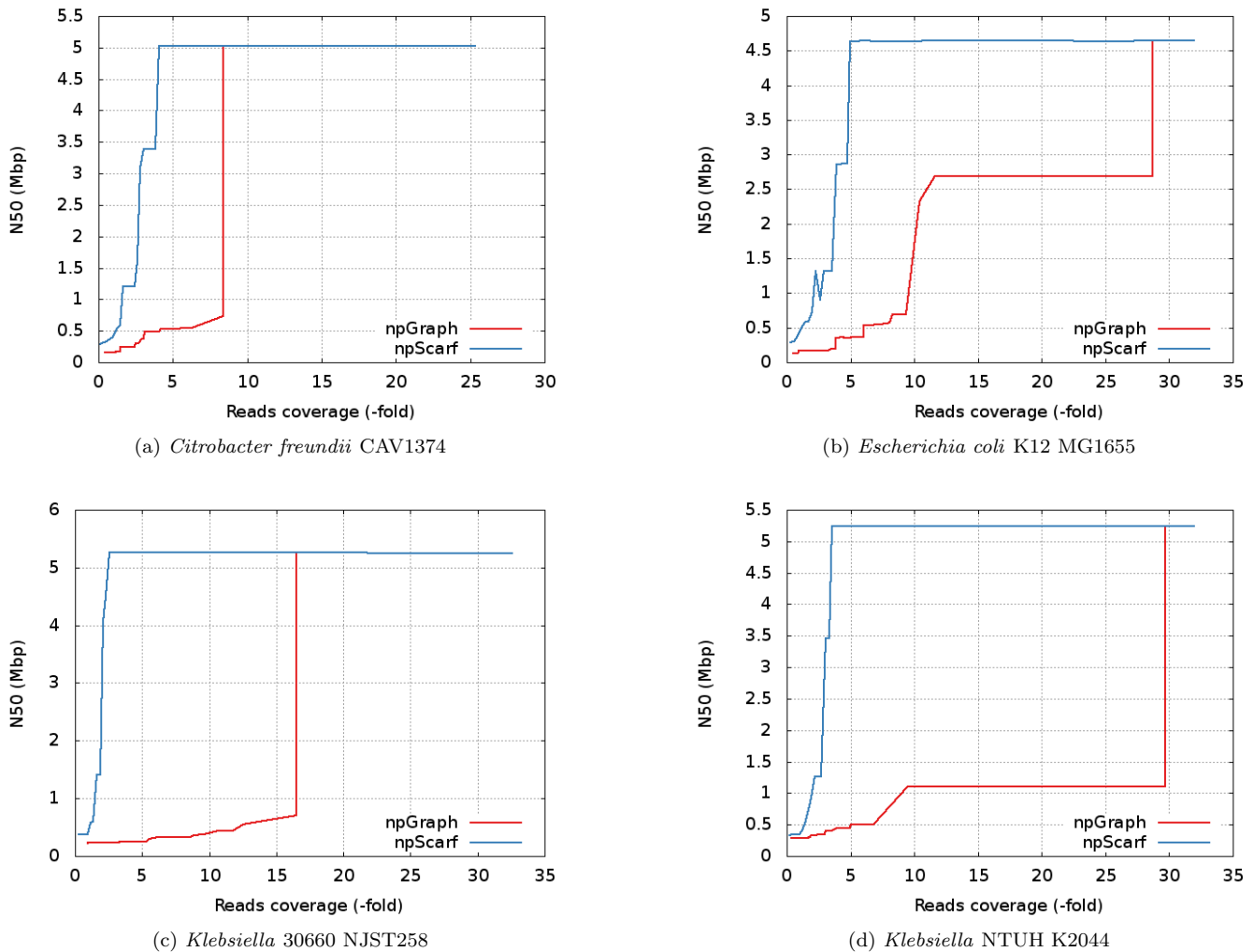


Figure 2: N50 statistics of real-time scaffolding by **npScarf** versus **npGraph**.

As can be observed from all the plots, **npGraph** and **npScarf** both converged to the same ultimate completeness but with different paces and patterns. Apparently it took more data for **npGraph** to finish the same genome than the other. The reason stems from the fact that the new algorithm implemented a more ‘conservative’ approach of bridge construction with at least 3 supporting long-reads for each to prevent any potential mis-bridging. Unlike **npScarf** when the connections could be undone and rectified later if needed, a bridge in **npGraph** will remain unchanged once created.

The plot for *E. coli* data clarifies this behaviour when a fluctuation can be observed in **npScarf** assembly at  $\simeq 3$ -folds data coverage. On the other hand, the N50 length of **npGraph** is always a monotonic increasing function. The sharp *jumping* patterns suggested that the linking information from long-read data had been stored and exploited at certain time point decided by the algorithm. Once a unique path has been determined, the bridge can be formed to connect the fragments together into longer sequences.

## Metagenomics assembly

We further employed **npGraph** on mock community data to study the performance of our method in metagenomics co-assembly problem. In this application, sequencing data (including both short and long reads) from mixtures of ten microbial species of ZymoBIOMICS Microbial Community Standards [22] were used as input for **npGraph**. The total genome size was estimated as 61.96 Mbp. There were two settings for the input depending on the distribution of cell abundances in the mixture itself, namely even and log population. On the other hand, 8 out of 10 genomes being sequenced were reconstructed by using PacBio sequencing (RSII and Sequel) previously [23], including *Bacillus subtilis*, *Enterococcus faecalis*, *Escherichia coli*, *Listeria monocytogenes*, *Pseudomonas aeruginosa*, *Saccharomyces cerevisiae*, *Salmonella enterica* and *Staphylococcus aureus*. We evaluated the coassembly results by running **metaQUAST** given 8 PacBio assembly as references.

Table 3: NGA50 improvement from **metaSPAdes** to **npGraph** assembly on two mock communities ZymoLog and ZymoEven. The statistics were generated by **metaQUAST** v3.2 with 8 (out of 10) available PacBio references of individual isolates [22].

Community	ZymoEven		ZymoLog	
	metaSPAdes	npGraph	metaSPAdes	npGraph
<i>B. subtilis</i>	23,386	382,368	35,390	433,078
<i>E. coli</i>	34,776	1,108,989	—	—
<i>E. faecalis</i>	23,340	217,908	—	—
<i>L. monocytogenes</i>	26,480	520,012	23,146	130,284
<i>P. aeruginosa</i>	59,372	1,753,658	161,816	444,495
<i>S. aureus</i>	26,058	175,908	—	—
<i>S. cerevisiae</i>	—	—	—	—
<i>S. enterica</i>	33,363	4,242,458	—	—

To run **npGraph** on the metagenomics data set, we firstly augmented binning information from using **metaBAT** [24] on the Illumina raw reads, before applying our method to the assembly graph generated by **metaSPAdes**. The default parameter setting was remained as it was for isolate assembly.

In terms of Illumina data, Even community had been sequenced by MiSeq platform which generated about 43-fold coverage while the Log community’s short-read data had been obtained from an Illumina HiSeq 1500, for about 156X coverage. Even though the total amount of base coverage from the latter was almost four-times richer than the former, its **metaSPAdes** assembly quality was lesser. This due to the fact of under-presented microbial cells from rare species in the log population that require much more input to compensate, resulting in significant smaller size of assembly contigs and more fragmented assembly graph (Supplementary Figure 3).

Table 3 shows the assembly improvement in terms of NGA50 after running **npGraph** on the **metaSPAdes** initial graph. As expected from better quality assembly graph, the results for the Even community indicated significant more complete genomes recovered. There were 7 isolate genomes had been identified for this community, compared to only 3 from the more complicated log population. **npGraph** had been able to resolve the assembly graph efficiently for Even community, with the maximum NGA50 improvement for *S. enterica* from 33 Kbp to 4.2 Mbp. On the other hand, genomes from the Log community witnessed increasing length of aligned contigs as well, but not as huge as the other. The longest NGA50 contigs belongs to *P. aeruginosa* of 445 Kbp, however, the counterpart from the Even community was 4-fold than that, at 1.75 Mbp. The only exception was *B. subtilis*, where **npGraph** can only resolved 382 Kbp correct length from the zymo even while the respective figure was 433 Kbp for the zymo log. It is noteworthy that for this case, initially the **metaSPAdes** assembly for the former was slightly better compared to the latter.

## Conclusions

Assembly graph is the data structure describing the assembly components at more details. The current chapter brings this informative knowledge to the original **npScarf**’s mechanism in two ways, either partly for the gap-filling module only (**npScarf\_wag**) or completely as the building block for the assembly construction method (**npGraph**).

While the first approach showed improvements in terms of base’s accuracy for the final results, it had limited ability in rectifying the mis-assemblies from the original version due to false positive alignments at contig level. The issue can be tackled by applying the assembly graph completely as in **npGraph**. With a more conservative bridging method applied, the new method may consume more data to confidently construct the assembly but at the same time, the number of

mis-located fragments has reduced significantly. Furthermore, users can monitor the assembly in an interactive manner providing the assembly GUI.

Compared to the other hybrid assemblers of similar methodology, such as **hybridSPAdes** and **Unicycler**, there are still rooms for further development of **npGraph**. More comprehensive pre-processing step is needed for a better input graph possible since it would affect the completeness of final results.

Importantly, a robust real-time voting system should be implemented to be able to detect the most probable path amongst all candidates in an efficient way. This would alleviate the data consumption of the **npGraph** while at the same time, maintain high confident and accurate scaffolding.

## Methods

Basically the work flow of **npGraph** consists of 3 main modules: (1) assembly graph loading and preprocessing; (2) graph resolving; (3) postprocessing and reporting results. The first step is to load the graph of Illumina contigs and retrieve their metadata which are helpful for the next steps, *e.g.* binning and multiplicity estimation. By using this information, in combination with path inducing from long reads, the assembly graph is then traversed and resolved in real-time. Finally, the graph is subjected to the last attempt of resolving and cleaning, as well as output the final results. The whole process can be managed by using either command-line interface or GUI. Among three phases, only the first one must be performed prior to the MinION sequencing process in a streaming setup. The algorithm works on the assembly graph of Illumina contigs, so the terms *contigs* and *nodes* if not mentioned specifically, would be used interchangeable throughout this context.

### Contigs binning

Each population is expected to include contigs of the similar abundance in the final assembly sequences, *e.g.* chromosome, plasmids, or even particular species genome in a metagenomics community. In addition, the binning phase would assist to differentiate between repetitive contigs and unique ones.

Each contig is represented as a single node in the assembly graph and an edge between two nodes indicate their overlap (link) properties. This step is to cluster the longest nodes (longer than 10Kbp) into different sets, namely *core* groups, based on the their degree (number of connections) and coverage values. DBSCAN clustering algorithm [25] is applied for this task by default. The rationale is to approximate a coverage value of a significant contig (which can be splitted into more than 10,000 *k-mers*) to be a sampled mean of a Poisson distribution (of *k-mers* count). The metric is a distance function based on Kullback-Leibner divergence [26], or relative entropy, of two Poisson distributions. Other than that, external binning tools can be employed for more complicated binning task, *e.g.* metagenomics, and the results can be integrated into **npGraph** for better performance. More details can be found on Supplementary Note 1.

### Multiplicity estimation

Due to the possible divergence of sequencing coverage relative to the real abundance of sequences, especially for the shorter contigs, an optimization step is carried out to alleviate this issue as shown in Supplementary Note 2. The coverage measures of nodes (which represent contigs) are propagated throughout the graph via connecting edges for calibrations prior to the multiplicity estimation.

Based on the coverage values of all the edges and the graph's topology, we induce the copy numbers of every significant nodes (long contigs) in the final paths. For each node, this could be done by investigating its adjacent edges and answering the questions of how many times it should be visited, from which abundance groups. Multiplicities of insignificant nodes (of sequences with length less than 1,000 bp) can be estimated in the same way but usually with less confident due to more complicated connections and greater variation of coverage values. For that reason, in **npGraph**'s algorithm, they are only used as augmented information to calculate likelihood scores of candidate paths containing corresponding nodes.

### Building bridges in real-time

Bridge is the data structure designed for tracking the possible connections between two anchored nodes (of unique contigs) in the assembly graph. A bridge must start from a unique contig, or *anchor* node, and end at another when completed. Located inbetween are nodes known as *steps* and distances between them are called *spans* of the bridge. Stepping nodes are normally repetitive contigs and indicative for a path finding operation later on. In a complicated assembly graph, the more details the bridge, *a.k.a.* more steps inbetween, the faster and more accurate the linking path it would resolve. A bridge's function is complete when it successfully return the ultimate linking path between 2 anchors.

The real-time bridging method considers the dynamic aspect of multiplicity measures for each node, meaning that a *n*-times repetitive node might become a unique node at certain time point when its (*n* - 1) occurrences have been already identified in other distinct unique paths. Furthermore, the streaming fashion of this method allows the bridge constructions (updating steps and spans) to be carried out progressively so that assembly decisions can be made immediately after having sufficient supporting data. The detail implementation is addressed in Supplementary Note 4.

A bridge in **npGraph** has several completion levels. When created, it must be rooted from an *anchor node* which represents a unique contig (level 1). A bridge is known as fully complete (level 4) if and only if there is a unique path connecting its two anchor nodes from two ends.



## Path finding algorithm

Given a bridge with 2 anchors, a path finding algorithm is invoked to find all candidate paths between them. Each of these paths is given a score of alignment-based likelihood which are updated immediately as long as there is an appropriate long read being generated by the sequencer. As more nanopore data arrives, the divergence between candidates' score becomes greater and only the top-scored ones are kept for the next round. We implement a modified stack-based version utilizing Dijkstra's shortest path finding algorithm [27] to reduce the search space when using Depth-First Search (Supplementary Note 5).

It is worth noting that due to dead-ends, there not always exist a path in the assembly graph connecting two anchors as suggested by the alignments. In this case, if enough long reads coverage (20X) are met, a consensus module is invoked and the resulting sequence is contained in a *pseudo* edge.

## Assembly graph resolving in real-time

npGraph resolves the graph by reducing its complexity perpetually using the long reads that could be generated in real-time. Whenever a bridge is finished (with only one path left), the assembly graph is *transformed* or *reduced* by replacing its unique path by an composite edge and removing any unique edges (edges coming from unique nodes) along the path. The assembly graph would have at least one edge less than the original after the reduction. The nodes located on the reduced path, other than 2 ends, also have their multiplicities subtracted by one and the bridge is marked as finally resolved without any further modifications.

## Result extraction and output

npGraph reports assembly result in real-time by decomposing the assembly graph into a set of longest straight paths (LSP), each of the LSP will present a contig for the result (Supplementary Note 6).

The final assembly output contains files in both FASTA and GFA v1 format (<https://github.com/GFA-spec/GFA-spec>). While the former only retains the actual genome sequences from the final decomposed graph, the latter output file can store almost every properties of the ultimate un-masked graph such as nodes, links and potential paths between them.

## References

- [1] Rozov R, Goldshlager G, Halperin E, Shamir R (2017) Faucet: streaming de novo assembly graph construction. *Bioinformatics* 34(1):147–154.
- [2] Cao MD et al. (2017) Scaffolding and completing genome assemblies in real-time with nanopore sequencing. *Nature Communications* 8:14515.
- [3] Wick RR, Judd LM, Gorrie CL, Holt KE (2017) Unicycler: resolving bacterial genome assemblies from short and long sequencing reads. *PLOS Computational Biology* 13(6):e1005595.
- [4] Giordano F et al. (2017) De novo yeast genome assemblies from MinION, PacBio and MiSeq platforms. *Scientific reports* 7(1):3935.
- [5] Antipov D, Korobeynikov A, McLean JS, Pevzner PA (2016) hybridSPAdes: an algorithm for hybrid assembly of short and long reads. *Bioinformatics* 32(7):1009–1015.
- [6] Prjibelski AD et al. (2014) ExSPAnde: a universal repeat resolver for DNA fragment assembly. *Bioinformatics* 30(12):i293–i301.
- [7] Bankevich A et al. (2012) SPAdes: A New Genome Assembly Algorithm and Its Applications to Single-Cell Sequencing. *Journal of Computational Biology* 19(5):455–477.
- [8] Zerbino DR, Birney E (2008) Velvet: algorithms for de novo short read assembly using de Bruijn graphs. *Genome research* 18(5):821–9.
- [9] Simpson JT et al. (2009) ABySS: A parallel assembler for short read sequence data. *Genome Research* 19(6):1117–1123.
- [10] Cao MD, Ganesamoorthy D, Cooper MA, Coin LJM (2016) Realtime analysis and visualization of MinION sequencing data with npReader. *Bioinformatics* 32(5):764–766.
- [11] Nguyen SH, Duarte TP, Coin LJ, Cao MD (2017) Real-time demultiplexing Nanopore barcoded sequencing data with npBarcode. *Bioinformatics* 33(24):3988–3990.
- [12] Huang W, Li L, Myers JR, Marth GT (2012) ART: a Next-generation Sequencing Read Simulator. *Bioinformatics* 28(4):593–594.
- [13] Ono Y, Asai K, Hamada M (2012) PBSIM: PacBio Reads Simulator – Toward Accurate Genome Assembly. *Bioinformatics*.

- [14] Mikheenko A, Prjibelski A, Saveliev V, Antipov D, Gurevich A (2018) Versatile genome assembly evaluation with QUAST-LG. *Bioinformatics* 34(13):i142–i150.
- [15] Myers EW et al. (2000) A Whole-Genome Assembly of *Drosophila*. *Science* 287(5461):2196–2204.
- [16] Li H (2013) Aligning sequence reads, clone sequences and assembly contigs with BWA-MEM. p. 3.
- 5 [17] Li H (2016) Minimap and miniasm: fast mapping and de novo assembly for noisy long sequences. *Bioinformatics* 32(14):2103–2110.
- [18] Brudno M et al. (2003) Glocal alignment: finding rearrangements during alignment. *Bioinformatics* 19(suppl\_1):i54–i62.
- [19] George S et al. (2017) Resolving plasmid structures in Enterobacteriaceae using the MinION nanopore sequencer: assessment of MinION and MinION/Illumina hybrid data assembly approaches. *Microbial genomics* 3(8).
- 10 [20] Carattoli A et al. (2014) Plasmidfinder and pmlst: in silico detection and typing of plasmids. *Antimicrobial agents and chemotherapy* pp. AAC–02412.
- [21] Potter RF, D’souza AW, Dantas G (2016) The rapid spread of carbapenem-resistant Enterobacteriaceae. *Drug Resistance Updates* 29:30–46.
- 15 [22] Nicholls SM, Quick JC, Tang S, Loman NJ (2019) Ultra-deep, long-read nanopore sequencing of mock microbial community standards. *Gigascience* 8(5):giz043.
- [23] McIntyre AB et al. (2019) Single-molecule sequencing detection of n 6-methyladenine in microbial reference materials. *Nature communications* 10(1):579.
- [24] Kang DD, Froula J, Egan R, Wang Z (2015) MetaBAT, an efficient tool for accurately reconstructing single genomes from complex microbial communities. *PeerJ* 3:e1165.
- 20 [25] Ester M, Kriegel HP, Sander J, Xu X (1996) A density-based algorithm for discovering clusters in large spatial databases with noise. (AAAI Press), pp. 226–231.
- [26] Kullback S, Leibler RA (1951) On information and sufficiency. *The annals of mathematical statistics* 22(1):79–86.
- [27] Dijkstra EW (1959) A note on two problems in connexion with graphs. *Numerische mathematik* 1(1):269–271.